Site percolation threshold of composite square lattices and its agroecology applications

D. Rosales Herrera,[1] Jorge Velázquez-Castro,[1,*] A. Fernández Téllez,[1] Jesús F. López-Olguín,[2,3] and J. E. Ramírez[3,†]

[1]*Facultad de Ciencias Físico Matemáticas, Benemérita Universidad Autónoma de Puebla, Apartado Postal 165, 72000 Puebla, Pue., Mexico*

[2]*Herbario y Jardín Botánico, Vicerrectoría de Investigación y Estudios de Posgrado, Benemérita Universidad Autónoma de Puebla, Apartado Postal 165, 72000 Puebla, Pue., Mexico*

[3]*Centro de Agroecología, Instituto de Ciencias, Benemérita Universidad Autónoma de Puebla, Apartado Postal 165, 72000 Puebla, Pue., Mexico*

(Received 29 August 2023; accepted 1 December 2023; published 11 January 2024)

We analyze the percolation threshold of square lattices comprising a combination of sites with regular and extended neighborhoods. We found that the percolation threshold of these composed systems smoothly decreases with the fraction of sites with extended neighbors. This behavior can be well-fitted by a Tsallis q-Exponential function. We found a relation between the fitting parameters and the differences in the gyration radius among neighborhoods. We also compared the percolation threshold with the critical susceptibility of nearest and next-to-nearest neighbor monoculture plantations vulnerable to the spread of phytopathogen. Notably, the critical susceptibility in monoculture plantations can be described as a linear combination of two composite systems. These results allow the refinement of mathematical models of phytopathogen propagation in agroecology. In turn, this improvement facilitates the implementation of more efficient computational simulations of agricultural epidemiology that are instrumental in testing and formulating control strategies.

DOI: 10.1103/PhysRevE.109.014304

I. INTRODUCTION

Percolation theory is usually associated with the study of transport phenomena occurring through porous media [1–3]. This theory arises from the observations made by Broadbent when he was designing charcoal filters for gas masks and measuring their efficiency. Later, in collaboration with Hammersley, Broadbent concluded that transporting a fluid (or individual particles) through a random media with a certain fraction of open (or closed) bonds defines a new kind of diffusion process [4]. Between 1954 and 1957, the percolation theory was formalized and thenceforth studied as a mathematical framework based on geometry and probability [4–6]. In this theory, the simplest way of modeling a porous media is by means of a square lattice, wherein each cell is assigned to be occupied with probability p or empty with the complementary probability $1 - p$ [3,7]. This assignation is carried out independently of the occupation state of the neighbor cells. By construction, the transport phenomena can only occur across the occupied cells. Notice that for small p values, there are few occupied cells in the system, and then the transport phenomenon cannot take place. On the other hand, if p takes values close to 1, the occupied cells fill the system, mostly grouped in a single giant cluster, named the spanning cluster, that connects the system from one side to the opposite side. The emergence of the spanning cluster in the system guarantees that the transport phenomenon occurs. The fundamental problem to solve in percolation theory is determining the minimal probability value required for the emergence of the spanning cluster. This critical value is known as the *percolation threshold*, which should be estimated for each specific problem [8].

Percolation theory has a wide diversity of applications, ranging from the study of the formation of galactic structures to the description of the formation and properties of the quark-gluon plasma [8–11]. Moreover, the analysis of the connection properties of the graph defined by social interactions and the main epidemiological parameters of diseases shed light on the development of mobility public policies that avoid the spacial propagation of epidemics [12,13].

Recently, in Refs. [14–17], the authors proposed a novel application of percolation theory in agronomy as an agroecological strategy to prevent the dissemination of harmful phytopathogens on plantations. In particular, they analyze the propagation of *Phytophthora* (from Greek, literally meaning plant destroyer) zoospores, micro-organisms classified as oomycetes that cause epiphytic interactions with the most destructive effects that attack the root of plants and trees in every corner of the world [18]. These zoospores swim chemotactically toward the plants using flagella, which can disperse through water films or soil moisture, including those on the surface of plants [18,19]. Many species of *Phytophthora* can persist as saprophytes if the environmental conditions are not appropriate but become parasitic in the presence of susceptible hosts [20,21]. Damages produced by this phytopathogen primarily concentrate in the root of plants but also include rotting in seedlings, tubers, corms, the base of the stem, and other organs. The diseases caused by exposure to

*jorgevc@fcfm.buap.mx
†jhony.ramirezcancino@viep.com.mx

 ©2024 American Physical Society

Phytophthora generate tremendous losses in agronomy and forestry. Due to the physiology of the oomycetes, most fungicides or antibiotics have no effects on them, motivating the research on nonchemical strategies that minimize or mitigate the propagation of the pathogen [18,22,23].

On the other hand, in laboratory experiments or *in situ* observation, it has been noted that some plants manifest the disease after the exposition to the pathogen, while others do not get sick because some individuals can deploy defense mechanisms against the infestation process (resistant plants) [14,15]. There are no methods to distinguish what seed will grow as a resistant plant. This fact allows us to define the plant susceptibility χ as the probability of an individual getting ill after the interaction with the phytopathogen, which can be experimentally measured through the determination of the survival rate of exposed plants.

In the context of percolation theory, the problem of *Phytophthora* propagation on a plantation can be modeled as a transport phenomenon on a regular lattice [14,16]. These systems are proposed to be studied on square lattices for simplicity. In a first approach, the lattice spacing can be chosen as the maximal length distance that zoospores can travel before starving or entering a state of dormancy. This guarantees that the micro-organisms can be spread over the adjacent plants. Under these considerations, this problem is directly mapped to a propagation process occurring on a square lattice with nearest neighbors, wherein occupied sites correspond to susceptible plants.

Another relevant ingredient of this model is the fraction of cells with the pathogen presence at the beginning of the propagation process. These cells are assumed to be uniformly and randomly distributed on the plantation. The propagation process is started in these inoculated cells. By construction, the zoospores move only at the adjacent cells, and they reproduce if they reach a susceptible plant. On the contrary, the zoospores die or enter into a dormancy state if they arrive at a resistant plant or an empty cell. However, the inoculated cells at the beginning of the propagation process have a fascinating behavior if they are adjacent to a susceptible plant and simultaneously occupy empty cells or cells with resistant plants. Under this condition, the inoculated cells act as bridges, connecting plants beyond the neighborhood definition, as we depict in Fig. 1 for square lattices with nearest and next-to-nearest neighbors. Moreover, the authors of Refs. [15,16] suggest that the systems look like a square lattice with regular sites together with a fraction of sites with an extended neighborhood. The latter fact motivates the work presented in this manuscript, wherein we explore the modifications of the percolation threshold due to the existence of sites with an extended neighborhood in the lattice.

In this work, we introduce the model of site percolation with a combination of two different nearest neighbor definitions, one with a neighborhood more extended than the other. These sites with extended neighborhoods play a similar role to the inoculated cells under the conditions described above. In the same way as in the percolation-agroecological model, the number of extended sites is controlled by the probability I. We compute the percolation threshold through computer simulations for a wide range of neighborhood combinations and I ranging from 0 to 1.

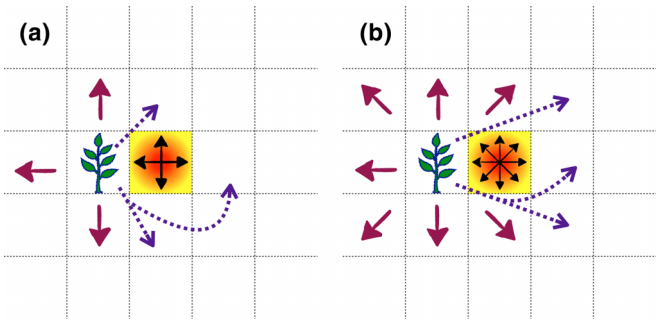

FIG. 1. Sketch of the interaction of an inoculated empty cell adjacent to a susceptible plant on (a) 2N and (b) 3N plantations. Despite *Phytophthora* zoospores moving accordingly to the neighbor definition (solid arrows), they can connect susceptible plants beyond the vicinity (dotted arrows), forming bridges that promote the formation of the spanning cluster.

The plan of the paper is as follows. In Sec. II, we provide the simulation and data analysis methods. In Sec. III, we show our results of the percolation threshold for the systems of interest. In Sec. IV, we discuss the applications of composite systems to model the propagation of phytopathogens on plantations. Finally, Sec. V contains the discussion of our results, conclusions, and perspectives.

II. SIMULATION METHOD AND DATA ANALYSIS

We use the Newman-Ziff simulation scheme [24,25] to determine the site percolation threshold of composite square lattices. This algorithm consists of measuring a particular observable O_n after adding exactly n sites. Therefore, the average $\langle O \rangle$ is computed at a particular p value by convoluting the O_n determinations with the fluctuations of the occupation probability. In Fig. 2 we show the neighborhood definitions used in this work: (a) nearest neighbors (2N), (b) next-to-nearest neighbors (3N). For the sake of notation, we denote as Ext1, Ext2, and Ext3 the extended neighborhoods in Figs. 2(c), 2(d) and 2(e), respectively. We explore the percolation threshold of square lattices considering all the possible pair combinations of these nearest neighbor definitions. In what follows, for a given pair combination, we call extended sites those with the larger neighborhood; meanwhile, the sites with the smaller ones are named regular sites.

In the simulation, we randomly add site by site. Each added site is randomly chosen to be regular or extended with probabilities $1 - I$ and I, respectively. Since in the lattice there are sites with two kinds of neighborhood definitions, we must pay special attention to the clustering process, which is performed by using the Union-Find algorithm. To do this, we assign different labels to sites in the system. However, if two sites belong to the same cluster, we update their labels to have the same value. For each site added, we first check the occupation states of every cell in the regular vicinity, and the site is merged with the cluster to which the occupied neighbor sites belong. Then, the complementary extended neighborhood is checked, but the clustering process fulfills the following rules: (i) if the added site is regular, it is only merged with the occupied extended sites; (ii) otherwise, the added extended

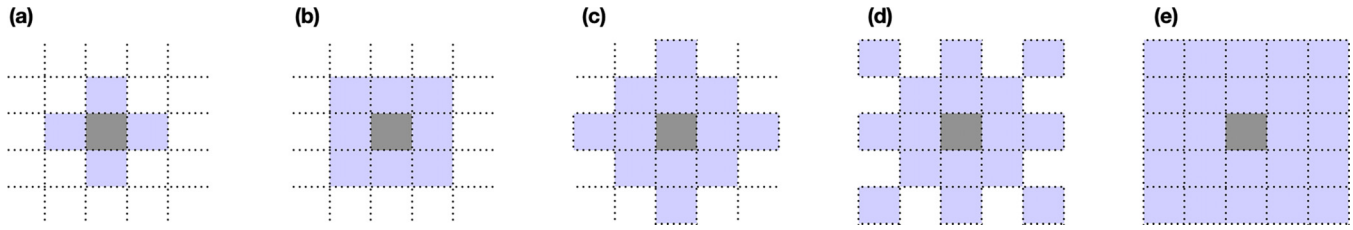

FIG. 2. Neighborhoods discussed in this manuscript: (a) 2N, (b) 3N, (c) Ext1, (d) Ext2, and (e) Ext3.

site is merged with all the occupied sites. In the simulation process, we consider systems with free boundary conditions.

The simulation is stopped when the spanning cluster emerges in the system. This occurs when, for the first time, sites on opposite sides of the lattice acquire the same label. At this point, we store the number of sites added. Using the information from 10^6 simulations, we construct the probabilities f_n and $F_n = \sum_{k=1}^{n} f_k$ of observing the emergence of the spanning cluster after adding exactly and at most n sites, respectively.

In the Newman-Ziff simulation scheme for a square lattice with L^2 sites, the average of an observable O at an arbitrary value of the occupation probability is computed as

$$O(p) = \sum_{n=1}^{L^2} O_n B(L^2, n, p), \tag{1}$$

where O_n is the value of the observable when there are exactly n occupied sites in the system, and $B(L^2, n, p)$ is the probability mass function of the binomial distribution, which counts the fluctuations of the number of occupied sites for a system filled with occupation probability p. Therefore, we compute the percolation probability by plugging the distribution F_n in (1), that is,

$$P_L(p) = \sum_{n=1}^{L^2} F_n B(L^2, n, p). \tag{2}$$

In Eq. (2), we have added the subscript L to denote the percolation probability dependence on the system size. To avoid the difficulties that carry the computation of the factorial of large numbers, we compute the binomial weights by using the following recursive formula [25]:

$$B(L^2, n, p) = \begin{cases} B(L^2, n-1, p)\frac{L^2-n+1}{n}\frac{p}{1-p} & \text{if} \quad n > n_{\mathrm{m}}, \\ B(L^2, n+1, p)\frac{n+1}{L^2-n}\frac{1-p}{p} & \text{if} \quad n < n_{\mathrm{m}}, \end{cases}$$

where $n_{\mathrm{m}} = pL^2$ is the n-value where the probability mass function of the binomial distribution takes its maximum value. Moreover, we set $B(L^2, n_{\mathrm{m}}, p) = 1$. In this way, the percolation probability (2) must be normalized by dividing by $\sum_{n=1}^{L^2} B(L^2, n, p)$.

After the computation of the percolation probability, the data set is fitted to the sigmoid function

$$P_L(p) = \frac{1}{2}\left[1 + \tanh\left(\frac{p - p_{cL}}{\Delta_L}\right)\right], \tag{3}$$

where p_{cL} is the estimation of the percolation threshold under the conditions of the systems in the simulation, and Δ_L is the width of the sigmoid transition [26]. To take into account finite-size effects on the percolation threshold, we perform simulations with different system sizes, $L = 32$, 48, 64, 96, 128, 192, 256, 384, and 512. Moreover, for each case under study, we determine the percolation threshold for a wide variety of values of the fraction of extended sites, starting at $I = 0$ until $I = 1$ with increments of $\Delta I = 0.05$. The data analysis is performed with the information of 10^6 simulations for each estimation of p_{cL}. In all cases, the well-known scaling relation $\Delta_L \propto L^{-1/\nu}$ for the width of the sigmoid transition is satisfied with $1/\nu \sim 0.75$, which is the universal value of the exponent corresponding to the correlation length found for 2D percolation systems [27].

Finally, we estimate the percolation threshold in the thermodynamic limit (p_c) by analyzing the scaling relation of $p_c - p_{cL}$ as a function of L. It has been previously observed that the free boundary conditions led to $p_c - p_{cL} \propto L^{-2/\nu}$ [10], which is a stronger finite-size effect than the universal scaling relation for the percolation threshold for finite lattices, given by $p_c - p_{cL} \propto L^{-1/\nu}$ [28]. We observe a good agreement of our data sets with the latter scaling relation. Therefore, we estimate the percolation threshold in the thermodynamic limit ($L \to \infty$) by extrapolating the trend of p_{cL} as a function of $L^{-2/\nu}$. In Sec. III, we summarize our estimations of the percolation threshold for all the possible combinations of neighborhood pairs depicted in Fig. 2.

III. RESULTS

We recall that there are sites with two different neighborhood definitions in the system. The number of each type of site is controlled by the parameter I. Given the value of I, the probability of adding a regular or extended site is $1 - I$ or I, respectively. Notice that there are two limit cases. When $I = 0$ or 1, only regular or extended sites are added to the system. These results are summarized in Table I. Our estimations of p_c for square lattices with 2N and 3N neighbors are in agreement with the best estimation of the percolation threshold reported in the literature. Moreover, for the extended neighborhoods

TABLE I. Percolation threshold, coordination number, and gyration radius of the neighborhoods discussed in this manuscript.

Neighborhood	Coordination number	p_c	R_g^2
2N [Fig. 2(a)]	4	0.592741(5)	4/5
3N [Fig. 2(b)]	8	0.40721(1)	4/3
Ext1 [Fig. 2(c)]	12	0.289117(9)	28/13
Ext2 [Fig. 2(d)]	16	0.20900(1)	60/17
Ext3 [Fig. 2(e)]	24	0.16466(2)	4

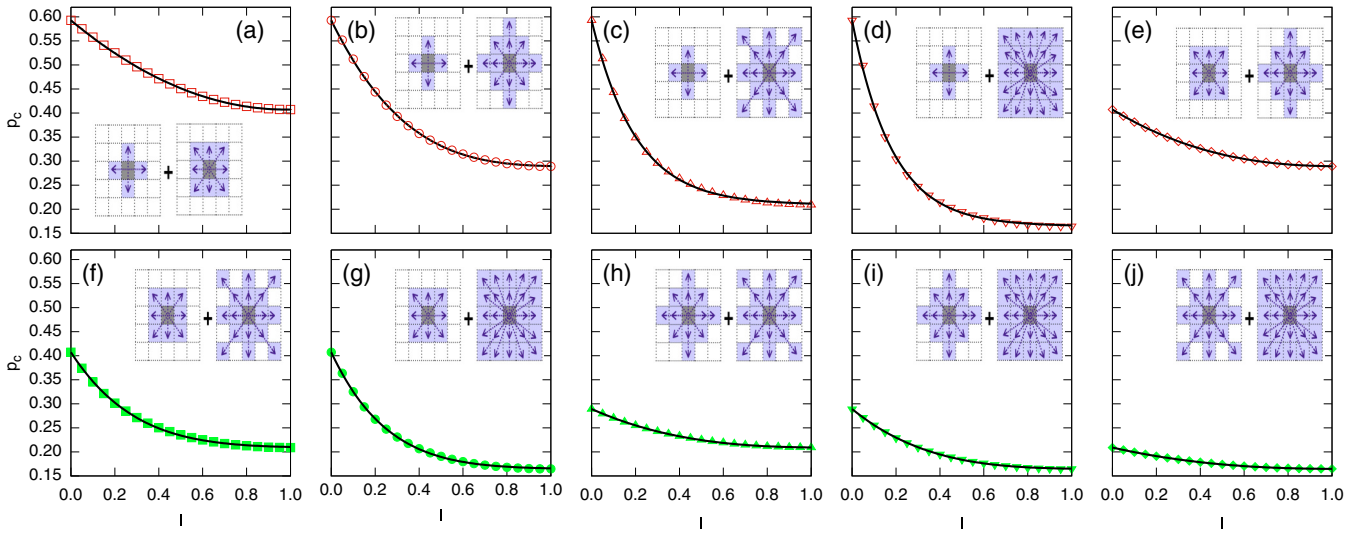

FIG. 3. Percolation threshold of composite square lattices (figures) together with their corresponding fitting function (solid lines). The neighborhood combinations are the following: (a) 2N+3N (empty red squares), (b) 2N+Ext1 (empty red circles), (c) 2N+Ext2 (empty red triangles), (d) 2N+Ext3 (empty red inverted triangles), (e) 3N+Ext1 (empty red diamonds), (f) 3N+Ext2 (filled green squares), (g) 3N+Ext3 (filled green circles), (h) Ext1+Ext2 (filled green triangles), (i) Ext1+Ext3 (filled green inverted triangles), and (j) Ext2+Ext3 (filled green diamonds).

Ext1, Ext2, Ext3, we have improved the previous estimations performed by Malarz in two digits [29,30].

In Fig. 3, we show our estimations of the percolation threshold in the thermodynamic limit for square lattices with a combination of regular and extended sites as a function of I. In all cases, p_c smoothly decreases from $p_{c,\mathrm{reg}}$ to $p_{c,\mathrm{ext}}$ as I increases, where $p_{c,\mathrm{reg}}$ and $p_{c,\mathrm{ext}}$ denote the percolation threshold for square lattices with only regular or extended sites, respectively. Despite the fact that the mean coordination number of the composite system $\bar{z} = z_{\mathrm{reg}} + I(z_{\mathrm{ext}} - z_{\mathrm{reg}})$ has a linear dependence on I, the percolation threshold for these systems does not response linearly nor inversely as a function of I. Notice that, at low values of the fraction of extended sites, the percolation threshold rapidly varies from $p_{c,\mathrm{reg}}$ because of the presence of the extended sites. In fact, p_c decays exponentially for low values of I, as further discussed below. On the contrary, for values of I close to 1, p_c asymptotically reaches the value of $p_{c,\mathrm{ext}}$, which means that the connectivity of the system is primarily due to the extended sites.

Additionally, we found that the percolation threshold of the system with combined neighbor definitions can be well fitted with a Tsallis q-Exponential function

$$p_c = p_{c,\mathrm{ext}} + (p_{c,\mathrm{reg}} - p_{c,\mathrm{ext}})\left(1 - \frac{I}{\lambda n}\right)^n, \tag{4}$$

where $n = 1/(1-q)$ defines the q parameter of the Tsallis function. In particular, for the cases 2N+Ext2 and 2N+Ext3, it is found that n takes large values; thus, we replace the Tsallis q-Exponential function for an exponential function. Table II summarizes the value of the fitting parameters for the cases discussed in this paper. The obtained fitting functions are shown as solid lines in Fig. 3. It is worth mentioning that the obtained n-values lead to $q < 1$, so the range of the fitting function is restricted to be $I < \lambda n$ [31], for which in almost all cases it occurs that $\lambda n > 1$, except for the combination 2N+3N. In this case, we obtain $\lambda n \approx 0.98$, and p_c takes complex values for $I > 0.98$. However, the imaginary part of p_c is of the order of 10^{-6} for $0.98 < I \leqslant 1$, which can be neglected, and the fitting function is extended to the rest of the interval [0,1] by taking the real part of (4).

Note that the series expansion of (4) around $I = 0$ approximates the Tsallis q-Exponential to an exponential decay given by

$$p_c - p_{c,\mathrm{ext}} \propto 1 - \frac{I}{\lambda} + O(I^2) \approx e^{-I/\lambda}, \tag{5}$$

where the factor $1/\lambda$ is the decay constant. In Fig. 4, we show this exponential behavior for all the neighborhood combinations discussed in this manuscript. In some instances, the p_c curve is scaled by a factor of 10^A to improve visualization. Note the agreement of the estimated percolation threshold for low values of I with the exponential function with a constant decay $1/\lambda$, where λ is taken from Table II.

TABLE II. Fit parameter values obtained for the percolation threshold of all the composite systems discussed in this manuscript.

Neighborhood	λ	n
2N+3N	0.488(7)	2.01(2)
2N+Ext1	0.33(1)	3.8(1)
2N+Ext2	0.201(1)	> 10
2N+Ext3	0.183(1)	> 10
3N+Ext1	0.428(5)	2.54(3)
3N+Ext2	0.28(3)	6.7(5)
3N+Ext3	0.25(3)	9.0(8)
Ext1+Ext2	0.40(1)	2.95(7)
Ext1+Ext3	0.33(1)	4.0(1)
Ext2+Ext3	0.432(5)	2.48(2)

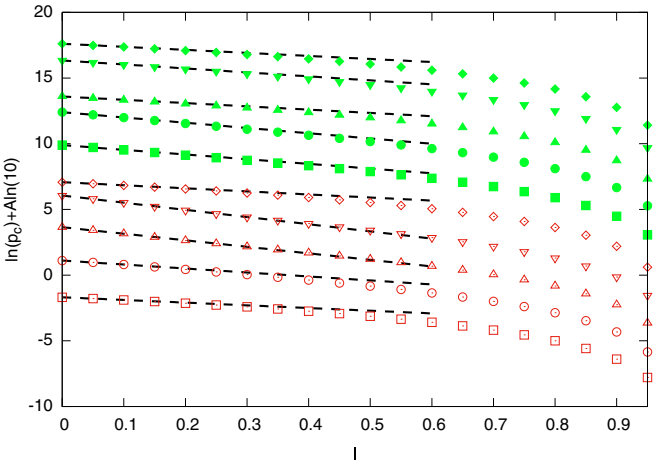

FIG. 4. Exponential behavior of composite systems at low values of I (figures) together with their exponential approximation (dashed lines). Figures and colors are the same as in Fig. 3.

Moreover, we found relationships between the fitting parameters and the difference in the radius of gyration of the extended and regular neighborhoods (see Fig. 5) as follows:

$$\lambda = c_2 e^{-c_1(R_{\mathrm{g,ext}} - R_{\mathrm{g,reg}})}, \tag{6}$$

$$\frac{1}{n} = m(R_{\mathrm{g,ext}} - R_{\mathrm{g,reg}}) + b, \tag{7}$$

with $c_1 = 1.13(3)$, $c_2 = 0.62(2)$, $m = -0.62(4)$, and $b = 0.61(3)$. $R_{\mathrm{g,ext}}$ and $R_{\mathrm{g,reg}}$ are the gyration radius of the extended and regular neighborhoods, respectively. The gyration radius is computed as

$$R_g^2 = \frac{1}{z+1} \sum_k z_k r_k^2, \tag{8}$$

where z_k is the number of possible neighboring sites at a distance r_k from the center of the figure, and z is the coordination number. In Table I, we show the values of R_g^2 for the neighborhood definitions under study. For the cases 2N+Ext2 and 2N+Ext3, we take $1/n \to 0$. In Sec. IV, we discuss how our results could be useful for understanding and modeling the propagation of phytopathogens on plantations.

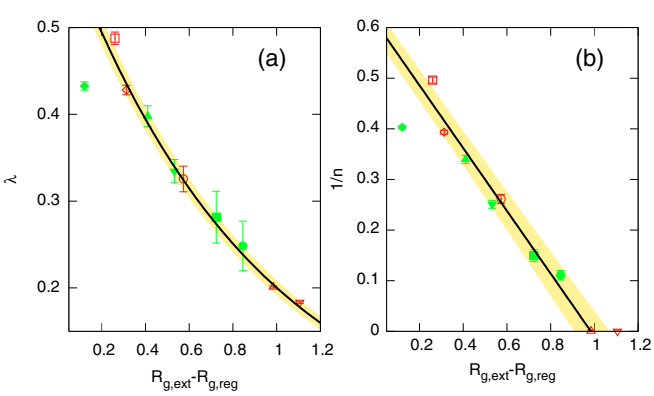

FIG. 5. Trend of the fit parameters (a) λ and (b) $1/n$ as functions of the difference in the neighborhood gyration radius of composite systems (figures). Solid lines correspond to the fitting functions of Eqs. (6) and (7), respectively. Shaded regions are the error propagation of the fitting functions. Figures and colors are the same as in Fig. 3.

IV. APPLICATION TO AGROECOLOGY

The propagation of *Phytophthora* zoospores has been previously studied as a percolation problem in Refs. [14–16]. In these studies, the authors discussed the characteristics needed for the formation of a spanning cluster of diseased and susceptible plants. The latter situation marks the onset of the outbreak on the plantation. It was shown that the percolation threshold depends substantially on the geometry of the plantation and the percentage of inoculated cells at the beginning of the propagation process. Inoculated sites that, at the same time, are empty or occupied with a resistant plant play the role of bridges connecting sites further away from the neighborhood definition.

Let us comment on the computational implementation for a monoculture plantation. The plantation is modeled as a regular lattice where its cells are assigned two independent occupancy states: inoculation and occupation by a susceptible plant. In this way, it is convenient to designate the cells containing active phytopathogens at the beginning of the propagation process. These inoculated cells are considered uniformly distributed and independent of the inoculated states of their neighbors. Then, using the Newman-Ziff algorithm, susceptible plants are added one by one. The clustering process between adjacent cells satisfies the following rules: (i) both sites are occupied with susceptible plants, or (ii) the neighboring site is inoculated. Although they are simple rules, the presence of the inoculated cells has a relevant impact on the formation of clusters, and thus on the percolation threshold. The simulation is stopped with the emergence of the spanning cluster of susceptible or diseased plants. The estimation of the percolation threshold is carried out by analyzing the generated data. Figure 6 shows the results of the percolation threshold as a function of the percentage of inoculated cells at the beginning of the propagation process for a plantation configured by square lattices with nearest and next-to-nearest neighbors, previously reported in Refs. [15,16].

In the context of this model, the *Phytophthora* propagation can only occur on susceptible plants, so the susceptibility takes the role of the occupation probability of traditional percolation lattices. Therefore, the percolation threshold is directly associated with the critical susceptibility χ_c of the plants. This means that the plantation should be sowed with plants having a susceptibility less than χ_c to avoid the outbreak. Similarly to the cases of square lattices with a fraction of extended neighbors, the critical susceptibility decreases as I grows. It is worth mentioning that there exists a minimal susceptible value that allows sowing the entire plantation even when all the cells are inoculated. However, considering that *Phytophthora* can survive under adverse environmental conditions, the management of the plantation is crucial in order to prevent outbreaks in future farming cycles.

We recall that this agroecological model connects sites over the regular neighborhood definition. However, the percolation threshold evolves similarly to square lattices with a fraction of extended neighbor sites. Here, the regular sites

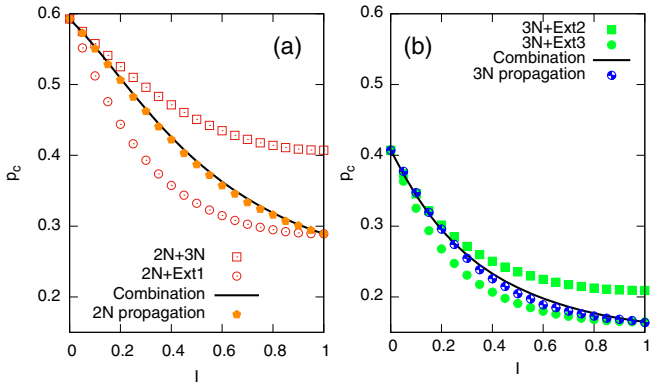

FIG. 6. Comparison between the percolation threshold of composite square lattices, the critical susceptibility of the agroecological model, and the linear combination approximation of Eqs. (9) and (10) (solid lines). (a) Case of 2N plantations. Squares and circles are the percolation thresholds of 2N+3N and 2N+Ext1 composite systems, respectively. Pentagons are the critical susceptibility of the agroecological model. (b) Case of 3N plantations. Squares and circles are the percolation thresholds of 3N+Ext2 and 3N+Ext3 composite systems, respectively. Semifilled circles are the critical susceptibility of the agroecological model.

correspond to the neighborhood definition used for clustering. Meanwhile, the extended sites must be determined by analyzing how the presence of the inoculated cells modifies the neighbor definition to connect susceptible plants, as depicted in Fig. 1. In what follows, we refer to 2N and 3N plantations as those sowed in a configuration based on 2N and 3N neighborhoods, respectively. Particularly for 2N and 3N plantations, we determine that the extended neighborhoods are 3N and Ext2 at low I-values but become Ext1 and Ext3 at high I-values, respectively.

Notice that the critical susceptibilities for 2N and 3N plantations are bounded as follows (see Fig. 6):

$$p_{c,\mathrm{2N+3N}} \leqslant \chi_{\mathrm{2N}} \leqslant p_{c,\mathrm{2N+Ext1}},$$

$$p_{c,\mathrm{3N+Ext2}} \leqslant \chi_{\mathrm{3N}} \leqslant p_{c,\mathrm{3N+Ext3}},$$

where $p_{c,\mathrm{reg+ext}}$ denotes the percolation threshold for the combination of neighborhoods reg and ext. For the sake of notation, we indicate the critical susceptibility by χ. Moreover, we found that the critical susceptibilities can be well-reproduced by the following linear combinations:

$$\chi_{\mathrm{2N}} = (1-I)p_{c,\mathrm{2N+3N}} + I p_{c,\mathrm{2N+Ext1}}, \tag{9}$$

$$\chi_{\mathrm{3N}} = (1-I)p_{c,\mathrm{3N+Ext2}} + I p_{c,\mathrm{3N+Ext3}}. \tag{10}$$

Equations (9) and (10) are shown in Fig. 6 as solid lines. We also find an exponential behavior for the critical susceptibilities at low I values:

$$\chi_{\mathrm{2N}} \propto 1 - \frac{I}{\lambda_1'} + O(I^2) \approx e^{-I/\lambda_1'}, \tag{11}$$

$$\chi_{\mathrm{3N}} \propto 1 - \frac{I}{\lambda_2'} + O(I^2) \approx e^{-I/\lambda_2'}, \tag{12}$$

where

$$\lambda_1' = \frac{\lambda_{\mathrm{2N+3N}}}{1 - \frac{p_{c,\mathrm{3N}}}{p_{c,\mathrm{2N}}}} \quad \text{and} \quad \lambda_2' = \frac{\lambda_{\mathrm{3N+Ext2}}}{1 - \frac{p_{c,\mathrm{Ext2}}}{p_{c,\mathrm{3N}}}}. \tag{13}$$

By discussing the case of 2N plantations, we now illustrate the applicability of Eqs. (9) and (10). Equation (9) indicates that the combinations 2N+3N and 2N+Ext1 are picked with probabilities $1-I$ and I, respectively. By construction, the regular and extended sites are also determined with probabilities $1-I$ and I, respectively. All the possibilities combine to give the probabilities $1-I$, $I(1-I)$, and I^2 of the added site has vicinity 2N, 3N, and Ext1, respectively. In the limit of low I, the added sites in simulations are mostly 2N, with a few ones with the 3N vicinity. As I rises, the number of sites with extended neighborhoods takes place and the percolation threshold decreases. In the limit of high I, the system is mainly formed by Ext1 sites. At this point, the system becomes homogeneous, and the critical susceptibility approaches $p_{c,\mathrm{2N+Ext1}}$. Using this framework, all the effects of inoculated cells are taken into account at once by incorporating sites with extended neighborhoods. Note that Eqs. (9) and (10) imply that composite systems discussed in this manuscript accurately describe the agroecology model in the limits $I=0$ and 1. Nevertheless, this model resembles percolation systems comprising three neighbor definitions for intermediate I values. Therefore, agroecological applications can be described by a percolation system comprising more than two neighborhood definitions.

V. CONCLUSIONS

In this work, inspired by the problem of the propagation of *Phytophthora* zoospores on plantations, we introduced a percolation model on square lattices that includes sites with a combination of two different neighborhood definitions. In particular, we explore all possible pair combinations of five neighborhoods that extend beyond the next-to-nearest definition, which are depicted in Fig. 2. By using computational simulations, we estimate the percolation threshold for all those systems as a function of the fraction of sites with extended vicinity.

We found that the percolation threshold of systems with combined neighborhoods smoothly decreases from $p_{c,\mathrm{reg}}$ to $p_{c,\mathrm{ext}}$, which can be well-fitted by the q-Exponential function as seen in Eq. (4). In the limit of low values of the fraction of sites with the extended neighborhood, the percolation threshold exponentially decays with I, where the rate constant is the inverse of the scale (λ) of (4). Moreover, we related the q-Exponential parameters to the differences in the radius of gyration between the regular and extended neighborhoods. Explicitly, $\lambda \propto e^{-m(R_{g,\mathrm{ext}}-R_{g,\mathrm{reg}})}$ and $1/n \sim (R_{g,\mathrm{ext}} - R_{g,\mathrm{reg}})$. However, the latter relations may no longer be valid for combinations with very small differences in the radius of gyration, as in the case of the combination Ext2+Ext3, whose fitting parameters deviate from the trend of the other cases. Further analysis is required to corroborate this hypothesis for systems with neighborhoods extended beyond those discussed in this manuscript.

Additionally, we compared our estimations of the percolation threshold with the results reported for the critical susceptibility of monoculture plantations. In the context of the agroecological model, I corresponds to the fraction of inoculated cells at the beginning of the propagation process. Similar to the extended sites in the model presented in this

manuscript, these cells act as bridges that connect susceptible plants beyond the neighbor definition of the lattice that models the plantation when they are placed in empty cells or with a resistant plant. It is worth mentioning that the critical susceptibilities for 2N and 3N plantations are well-described by the linear combinations [see Eqs. (9) and (10)] of the percolation threshold of the composites 2N+3N and 2N+Ext1 and 3N+Ext2 and 3N+Ext3 (see Fig. 6), respectively. We also found that the critical susceptibility behaves as an exponential decay in the limit of low values of I. In Eq. (13) we report the decay constant for 2N and 3N plantations. Note that the agroecological model can also motivate the study of systems with more than two extended neighborhoods.

This work can be broadened in different directions. One possibility is to consider other regular lattices, for instance the triangular or the honeycomb. Analyzing the bond or the joint site-bond percolation model under this approach would be meaningful. Another possibility consists of including the linear combination approach in more complex situations, for example in polyculture or structured plantations. It is worth noticing that all these perspectives are inspired by the agroecological model.

ACKNOWLEDGMENTS

This work was funded by Consejo Nacional de Humanidades, Ciencias y Tecnologías (CONAHCYT-México) under Project No. CF-2019/2042, graduated fellowships Grant No. 1140160, and postdoctoral fellowship Grant No. 289198. The authors thankfully acknowledge the computer resources, technical expertise, and support provided by the Laboratorio Nacional de Supercómputo del Sureste de México, CONAHCYT member of the network of national laboratories.

[1] J. M. Hammersley, Ann. Math. Stat. **28**, 790 (1957).
[2] H. L. Frisch and J. M. Hammersley, J. Soc. Ind. Appl. Math. **11**, 894 (1963).
[3] D. Stauffer and A. Aharony, *Introduction To Percolation Theory* (Taylor & Francis, Philadelphia, 2003).
[4] A. L. Efros, *Physics And Geometry of Disorder* (Mir, Moscow, 1982).
[5] B. Bollobás and O. Riordan, *Percolation* (Cambridge University Press, Cambridge, 2006).
[6] J. W. Essam, Rep. Prog. Phys. **43**, 833 (1980).
[7] G. Grimmett, *What is Percolation?* (Springer, Berlin, 1999).
[8] M. Sahimi, *Applications of Percolation Theory* (Taylor & Francis, Boca Raton, FL, 1994).
[9] P. E. Seiden and L. S. Schulman, Adv. Phys. **39**, 1 (1990).
[10] J. C. Texca García, D. Rosales Herrera, J. E. Ramírez, A. Fernández Téllez, and C. Pajares, Phys. Rev. D **106**, L031503 (2022).
[11] J. E. Ramírez, B. Díaz, and C. Pajares, Phys. Rev. D **103**, 094029 (2021).
[12] J. E. Ramírez, D. Rosales Herrera, J. Velázquez-Castro, B. Díaz, M. I. Martínez, P. Vázquez Juárez, and A. Fernández Téllez, Rev. Mex. Fis. **68**, 011701 (2022).
[13] M. Pardo-Araujo, D. García-García, D. Alonso, and F. Bartumeus, Sci. Rep. **13**, 11409 (2023).
[14] J. E. Ramírez, E. Molina-Gayosso, J. Lozada-Lechuga, L. M. Flores-Rojas, M. I. Martínez, and A. Fernández Téllez, Phys. Rev. E **98**, 062409 (2018).
[15] J. E. Ramírez, C. Pajares, M. I. Martínez, R. Rodríguez Fernández, E. Molina-Gayosso, J. Lozada-Lechuga, and A. Fernández Téllez, Phys. Rev. E **101**, 032301 (2020).
[16] D. Rosales Herrera, J. E. Ramírez, M. I. Martínez, H. Cruz-Suárez, A. Fernández Téllez, J. F. López-Olguín, and A. Aragón García, Chaos **31**, 063105 (2021).
[17] I. Taguas, J. A. Capitán, and J. C. Nuño, Phys. Rev. E **105**, 064301 (2022).
[18] K. Lamour, *Phytophthora: A Global Perspective* (CAB International, Croydon, UK, 2013).
[19] O. K. Ribeiro, Q. Rev. Biol. **54**, 187 (1978).
[20] R. C. Ploetz and J. L. Haynes, Proc. Fla. State Hort. Soc. **113**, 211 (2000).
[21] A. R. Hardham, Mol. Plant Path. **6**, 589 (2005).
[22] W. E. Fry and S. B. Goodwin, Plant Dis. **81**, 1349 (1997).
[23] A. J. Gevens, R. S. Donahoo, K. H. Lamour, and M. K. Hausbeck, Phytopathology **97**, 421 (2007).
[24] M. E. J. Newman and R. M. Ziff, Phys. Rev. Lett. **85**, 4104 (2000).
[25] M. E. J. Newman and R. M. Ziff, Phys. Rev. E **64**, 016706 (2001).
[26] M. D. Rintoul and S. Torquato, J. Phys. A **30**, L585 (1997).
[27] A. Coniglio, J. Phys. A **15**, 3829 (1982).
[28] R. M. Ziff, Phys. Rev. Lett. **69**, 2670 (1992).
[29] K. Malarz and S. Galam, Phys. Rev. E **71**, 016125 (2005).
[30] M. Majewski and K. Malarz, Acta. Phys. Pol. B **38**, 2191 (2007).
[31] G. Wilk and Z. Włodarczyk, Phys. Rev. Lett. **84**, 2770 (2000).